Published in final edited form as:
Eur J Neurosci. 2011 September ; 34(5): 695–704. doi:10.1111/j.1460-9568.2011.07799.x.

Modulation by the BK accessory β4 subunit of phosphorylation-dependent changes in excitability of dentate gyrus granule neurons

David Petrik, **Bin Wang**, and **Robert Brenner**
The University of Texas Health Science Center at San Antonio, Department of Physiology, 7703 Floyd Curl Drive, San Antonio, Texas 78229

Abstract

BK channels are large conductance calcium- and voltage-activated potassium channels critical for neuronal excitability. Some neurons express so called fast-gated, type I BK channels. Other neurons express BK channels assembled with the accessory β4 subunit conferring slow-gating of type II BK channels. However, it is not clear how protein phosphorylation modulates these two distinct BK channel types. Using β4 knockout mice, we compared fast- or slow-gated BK channels in response to changes in phosphorylation status of hippocampus dentate gyrus granule neurons. We utilized the selective PP2A/PP4 phosphatase inhibitor, Fostriecin, to study changes in action potential shape and firing properties of the neurons. In β4 knockout neurons, Fostriecin increases BK current, speeds BK channel activation, and reduces action potential amplitudes. Fostriecin increases spiking during early components of an action potential train. In contrast, inhibition of BK channels through β4 in wild type neurons or by BK channel inhibitor Paxilline opposes Fostriecin effects. Voltage clamp recordings of neurons reveal that Fostriecin increases both calcium and BK currents. However, Fostriecin does not activate BK α alone channels in transfected HEK293 cells lacking calcium channels. In summary, these results suggest that the fast-gating, type I BK channels lacking β4 can increase neuronal excitability in response to reduced phosphatase activity and activation of calcium channels. By opposing BK channel activation; the β4 subunit plays an important role in moderating firing frequency regardless of changes in phosphorylation status.

Keywords

phosphorylation; BK channels; β4 subunit; hippocampus; mouse

INTRODUCTION

Large conductance voltage- and calcium-activated potassium (BK) channels are unique due to their activation by coincident membrane depolarization and calcium influx (Cui *et al.*, 1997; Horrigan & Aldrich, 2002). BK channels generally sharpen the repolarization phase and contribute to the fast afterhyperpolarization (fAHP) of action potentials (Sah & Faber, 2002). Diversity of BK channels is conferred by β subunits that tailor BK channel properties to different cell types (Orio *et al.*, 2002). The neuron-specific β4 subunit inhibits BK channels by slowing activation (Behrens *et al.*, 2000; Brenner *et al.*, 2000a; Weiger *et al.*,

Correspondence to R. Brenner, Department of Physiology, UT Health Science Center at San Antonio, 7703 Floyd Curl Drive, San Antonio, Texas 78229, Phone 210-567-4343, Fax 210-567-4410, brennerr@uthscsa.edu.

Present affiliation for David Petrik is The University of Texas Southwestern Medical School, Department of Psychiatry, 5323 Harry Hines Boulevard, Dallas, Texas 75390-90702.

2000; Ha *et al.*, 2004; Wang *et al.*, 2009) and reducing their contribution to action potential repolarization (Brenner *et al.*, 2005; Wang *et al.*, 2009). Gain-of-function resulting from knockout of β4 causes increased firing frequency (Brenner *et al.*, 2005; (Martin *et al.*, 2008).

Neuronal BK channels recorded from synaptosomal membrane preparations were initially classified as fast-gated or slow-gated type BK channels (Reinhart *et al.*, 1989). Fast-gated BK channels are likely formed by the α subunits alone, whereas slow-gating is conferred by the β4 subunit (Meera *et al.*, 2000; Weiger *et al.*, 2000). These synaptosomal BK types were also correlated with distinct responses to phosphorylation (Reinhart *et al.*, 1991). Fast-gated BK channels seem to be activated by protein kinase A (PKA) and inhibited by protein phosphatase 2A (PP2A), whereas slow-gated BK channels have reduced activation by PKA that is reversed by PP2A (Reinhart *et al.*, 1991).

We wanted to confirm the phosphorylation phenotype to BK channels with or without the β4 subunit since the functional roles that different BK channel subtypes play in response to changes in phosphorylation status of neurons *in situ* have not been studied to date. This is partly due to the relatively non-selective action of most traditional phosphatase inhibitors and their broad target specificity. We have overcame this hindrance by using a novel phosphatase inhibitor Fostriecin that has four orders of sensitivity higher for PP2A and PP4 compared to other phosphatases (Lewy *et al.*, 2002). In addition, we were able to discern the fast- and slow-gating BK types by comparing β4 knockout mice to their wild type counterparts (Brenner *et al.*, 2005; Wang *et al.*, 2009). Our approach using a novel PP2A/PP4 inhibitor with β4 knockout mice thus offers a unique way to study the role of phosphorylation status on BK channels with or without the β4 subunit.

In this study we have investigated the role of β4 in BK channel response to changes in neuronal phosphorylation status. For the first time, we confirmed that the fast-gating BK channels in neurons are activated by PP2A/PP4 inhibition. Furthermore, we found that knockout of β4 sensitizes neurons to actions of PP2A/PP4 inhibitor Fostriecin. The consequences of Fostriecin are BK channel activation, truncation of action potential amplitude and increase spiking during early components of an action potential train. These results suggest a new role for β4 in normalizing BK channels response to increased phosphorylation status of neurons.

METHODS

Isolation of brain slices

All animal procedures were reviewed and approved by the University of Texas Health Science Center at San Antonio Institutional Animal Care and Use Committee (IACUC). Brain slices were prepared from 4–7 weeks old animals. β4 knockout (KO) mice were generated as described previously (Brenner *et al.*, 2005). Animals used for this study were inbred for 5 generations to C57BL/6J and compared to control wild-type (WT) C57BL/6J mice. In contrast to the original mixed 129svj/C57BL/6J background strain, the inbred C57BL/6J background fail to have spontaneous seizures. Therefore observed changes more likely represent direct effects of BK channels properties rather than indirect effects of seizures. Animals were fully anesthetized by Isoflurane (Butler Animal Health Supply, Dublin, OH, USA) prior to their sacrifice by decapitation. The whole brain was extracted from the skull in less than 1 minute and 15 seconds after decapitation and placed in ice-cold cutting solution containing (in mM) 2 KCl, 2 $MgSO_4$, 1.25 NaH_2PO_4, 1 $CaCl_2$, 2 $MgCl_2$, 26 $NaHCO_3$, 10 D-dextrose, 0.4 Vitamin C, and 206 Sucrose). The brain was than attached to a cutting platform and sliced (while constantly bubbled with 95% O_2/5% CO_2 mixture) to 400 μM thick coronal sections no later than 3–4 minutes after the brain extraction. The slicing was performed on a Leica VT1000S vibratome (Leica Microsystems, Bannockburn, IL,

USA) in ice-cold cutting solution. The brain slices recovered in 30 °C extracellular solution for 1 hour and then were kept at room temperature for at least another 1 hour prior to first measurements. The extracellular solution contained (in mM) 124 NaCl, 2 KCl, 2 $MgSO_4$, 1.25 NaH_2PO_4, 2 $CaCl_2$, 26 $NaHCO_3$, 10 D-dextrose and 0.4 mM Vitamin C.

Whole-cell current-clamp recordings

The above extracellular solution was also used for the patch-clamp experiments in the whole-cell configuration. The recordings were conducted at room temperature with an internal solution of (in mM) 120 potassium gluconate, 20 KCl, 2 $MgCl_2$, 10 HEPES, 2 ATP, 0.25 GTP and 0.1 EGTA (pH = 7.4; free calcium content was calculated to be approximately 50 nM using MaxC software (Patton, Stanford University)). To block PP2A, 250 nM Fostriecin (BioAustralis Products, Smithfield, NSW, Australia; 200-times dilution of the stock solution) was added to the internal solution. 50 μM frozen aliquots of Fostriecin were made from a lyophilized powder and used no longer than 3 weeks. To activate PKA, 1 mM cAMP (Sigma, St. Louis, MO, USA; pH = 7.4; 100-times diluted stock solution) was added to the internal solution. For paired experiments, intracellular application of 250 nM Fostriecin or 1 mM cAMP was combined with extracellular application of Paxilline in 5 μM final concentration. Paxilline was added into the extracellular (bath) solution in 1:2000 dilutions from its stock solution (10 mM in DMSO; Sigma, St. Louis, MO, USA). The brain slice was perfused with Paxilline for at least 15 minutes prior to first measurements.

Granule cells of the hippocampus were identified at 60X magnification using a water-submersible objective and DIC/infrared optics on a BX51WI Olympus microscope. Granule cells from the third to fifth layer (counting from the slice surface) were selected for patch clamping using the whole-cell mode of a HEKA EPC10 feedback amplifier and Patchmaster software (HEKA Instruments, Germany). Cells were used only if they maintained a resting membrane potential of at least −75 mV and if they had an input resistance of 300 MΩ or larger. Series resistance was compensated via the amplifier. If capacitance or series resistance changed by more than 20% during recordings, the cell was excluded from further analysis. A hardware filter of 3 kHz was used for data collection. Current-clamp recordings were performed from a holding current to maintain −80 mV, and stepping up using a series of rectangular current injections with 15 pA increments. The pulse protocol had a series of 30 steps (from 0 pA to 450 pA injections) and each current injection step was 1000 ms long. Trains of action potentials were measured three minutes after break-in into the whole-cell from a GΩ seal. This was done to allow Fostriecin or cAMP effects to take place. Similarly, controls were also measured three minutes after the break-in.

Measurement of Action Potentials

For evaluation of individual action potential properties, action potential waveforms elicited by the 210 pA current injection were used. Action potential waveform statistics were obtained from the average of the 10^{th} and 11^{th} action potential waveforms. AxoGraph software (Kagi, Berkeley, CA, USA) was used to characterize individual action potential waveforms properties. The action potential (AP) amplitude was measured from the threshold voltage to its maximum voltage. AP half-width was the width of action potential at the half-point of the peak amplitude. The amplitude of fAHP was measured from the threshold voltage to the most negative over-shoot after repolarization. The interspike voltage was measured at the half time between the amplitudes of the fourth and the fifth action potential peak to avoid taking into account the fAHP overshoot.

Intrinsic membrane properties were also measured. The input resistance (IR) was estimated using a current-clamp injection of −50 pA from an −80 mV holding current. The action potential threshold was a measurement of the first derivative of the voltage rise elicited by a

diagonal current injection of 125 pA over a 200 millisecond time period. Firing frequency (in Hz) was calculated as the number of action potential peaks (with amplitudes higher than 20 mV) over a period of 1 second. Instantaneous frequency was calculated as a reverse value of mean cumulative inter-event interval (in Hz) using the AxoGraph software (Kagi, Berkeley, CA, USA). All data are represented as mean ± SEM. Unpaired T-Test is used for statistical analysis. One asterisk represents $P < 0.05$, two represent $P < 0.01$, and three represent $P < 0.001$. Degrees of freedom is df. Data are presented and statistically analyzed using KaleidaGraph (Synergy Software, Reading, PA, USA), Excel (Microsoft, Redmont, WA, USA) and Igor Pro (WaveMetrics, Portland, OR, USA).

Whole-cell voltage-clamp recordings

The whole-cell voltage-clamp experiments were performed to measure BK and voltage-gated calcium currents. Whole-cell currents were elicited using voltage clamp steps from −80 mV to +110 mV in 10 mV increments. The pulses were 40 ms long and followed by steps down to −65 mV for 15 ms. Data were sampled at 10–30-μs intervals and low-pass filtered at 8.4 kHz using the HEKA EPC10 four-pole Bessel filter. Data were analyzed without further filtering. Leak currents were subtracted after the test pulse using P/5 negative pulses from a holding potential of −120 mV. Patch pipettes (borosilicate glass, World Precision Instruments, Sarasota, FL, USA) were coated with Sticky Wax (Kerr Corp., Romulus, MI, USA) and fire polished to 5–7 MΩ resistance.

For measuring the BK currents, brain slices were perfused with ACSF fluid containing 1 μM tetrodotoxin (TTX, 1:2000 dilution from a 2 mM stock solution of a citrate buffer, pH = 5, Sigma, St. Louis, MO, USA) to block voltage-dependent sodium channels. The internal solution had the same composition as the one used for the current-clamp experiments. Brain slices were perfused for at least 15 minutes prior to the first measurements. Controls where no Fostriecin was added were compared with cells containing 250 nM Fostriecin in the intracellular solution. Whole-cell currents were measured three minutes after break-in for both controls and Fostriecin-treated cells. After the currents were measured, the perfusion was switched from regular ACSF to ACSF containing 5 μM Paxilline (in 1:2000 dilution). The currents were recorded 10 minutes after switching into Paxilline-ACSF. The BK currents were obtained by subtracting the currents after Paxilline from currents before Paxilline in IGOR Pro software (WaveMetrics, Portland, OR, USA). Summary data represent the sustained BK component at +40 ms from the beginning of the depolarizing pulse. To obtain a current density measurement, the BK currents were divided by the individual whole-cell capacitances (in picoFarrads) measured by the EPC10 amplifier slow capacitance component. The cells that did not maintain the capacitance within ± 15% of the original value were not used for the analysis. Un-paired T-Test was used for the statistical analysis. One asterisk represents $P < 0.05$.

To measure voltage-dependent calcium currents, brain slices were perfused with ACSF containing several potassium and sodium channel blockers to remove contamination from their respective conductance. This ACSF (called ACSF-Ca) contained 10 mM tetraethyl-ammonium chloride (TEA-Cl, ICN Biomedicals Inc., Aurora, OH, USA), 5 mM 4-aminopyridine (4-AP), 5 mM cesium chloride and 1 μM TTX (all from Sigma, St. Louis, MO, USA). Osmolality and pH for ACSF-Ca was measured after thorough bubbling with 95%O_2/5%CO_2 mixture. The osmolality was 315 mOsm and pH was 7.4. The intracellular solution contained 141 mM cesium methane-sulfonate (Sigma, St. Louis, MO, USA) to replace KCl, and (in mM) 10 HEPES, 5 BAPTA, 2 Na-ATP, 0.25 GTP, 2 $MgCl_2$; pH = 7.31 and 310 mOsm. The controls were compared with cells perfused with the intracellular solution containing 250 nM Fostriecin three minutes after break-in. The maximum voltage-gated calcium currents were elicited by a series of rectangular depolarizing currents from −60 to +50 mV in a 10 mV increments lasting 200 ms. Prior to each 10 mV increment, the

cells were kept at −110 mV for 150 ms. The tail currents were elicited by stepping from a depolarizing current to −65 mV for 100 ms. The maximum amplitude of the inward currents was measured and divided by the whole-cell slow capacitance that was obtained as described previously. The cells that did not maintain the capacitance within ± 15% range of the original value were not used for the analysis. The whole-cell inward currents were inspected and traces that displayed delayed activation kinetics (due to space clamp problems) were removed from further analysis. Un-paired T-Test was used for the statistical analysis. One asterisk represents $P < 0.05$, two represent $P < 0.01$, and three represent $P < 0.001$.

To further confirm that the observed inward currents were indeed voltage-gated calcium currents, we performed paired experiments with cadmium chloride. Brain slices were treated the same as described above. After establishing a whole-cell configuration, the currents were measured three minutes after using the same depolarizing protocol that was described above. Following the control measurements ("before cadmium") in ACSF-Ca, the perfusion was switched into ACSF-Ca containing 20 μM cadmium chloride to block calcium currents. The perfusion with $CdCl_2$ resulted in about 95% reduction of the inward current. Paired T-Test was used for the statistical analysis. One asterisk represents $P < 0.05$, two represent $P < 0.01$, and three represent $P < 0.001$.

Recording of BK channels in HEK293 cells

The mouse α subunit cDNA (mB2 clone from mouse brain, GenBank/EMBL/DDBJ accession no. MMU09383, (Pallanck and Ganetzky, 1994)) in expression vector in pcDNA3 was used. Mouse BK channel α subunits were transfected into HEK 293T cells using 0.25–0.3 μg DNA and 10 μl Lipofectamine Reagent (Invitrogen, Carlsbad, CA, USA) per 35 mm dish of cells. For coexpression of β4, 1.5 μg mouse β4 cDNA was also added to the above mixture. After 4–5 hours of incubation, the cells were washed with PBS and re-plated on German glass coverslips (Bioindustrial Products, San Antonio, TX, USA) and analyzed by electrophysiology for the following 1–2 days. GFP expression from cotransfection (0.2 μg) of the EGFP-N1 plasmid (Clontech Laboratories, Inc., Mountain View, CA, USA) was used to identify cells expressing the channels. The cells were kept at 37°C in Dulbecco's Modified Eagle Medium (DMEM, Invitrogen, Carlsbad, CA, USA) with high D-glucose (4.5 g/l). DMEM was supplemented with 1% volume Penicillin-Streptomycin (100 U/ml, Cellgro, Lawrence, KS, USA), 10% volume fetal bovine serum (Invitrogen, Carlsbad, CA, USA) and 1% volume L-Glutamine (Invitrogen, Carlsbad, CA, USA).

Macroscopic current recordings were made using the patch-clamp technique in the inside-out configuration. Experiments were performed at room temperature. Data were sampled at 10–30-μs intervals and low-pass filtered at 8.4 kHz using the HEKA EPC10 four-pole Bessel filter. Data were analyzed without further filtering. Leak currents were subtracted after the test pulse using P/5 negative pulses from a holding potential of −120 mV. Patch pipettes (borosilicate glass, World Precision Instruments, Sarasota, FL, USA) were coated with Sticky Wax (Kerr Corp., Romulus, MI, USA) and fire polished to 3–5 MΩ resistance. The external recording solution (electrode solution) was composed of (in mM) 20 HEPES, 140 $KMeSO_3$, 2 KCl, 2 $MgCl_2$, pH 7.3. The internal solution was composed of a pH 7.3 solution of (in mM) 20 HEPES, 140 $KMeSO_3$, 2 KCl, and buffered with 5 HEDTA and added CaCl2 (VWR, West Chester, PA, USA) to the appropriate concentrations to give 4.0 μM estimated free Ca^{2+} concentration.

To measure effects of PP2A/PP4 inhibition in HEK293 cells, BK channel-transfected cells were kept in 250 nM Fostriecin (BioAustrailius Products, Smithfield, NSW, Australia) for 20 minutes in cell culture media (DMEM with 10% fetal bovine serum) at 37ºC. Cells were transferred to a recording chamber and patches were excised in internal solution (described

above) containing 250 nM Fostriecin. Conductance–voltage (G-V) relationships were obtained using a test pulse to positive potentials followed by a step to a negative voltage (–80 mV) and then measuring instantaneous tail current amplitudes 200 μs after the test pulse. Values for $V_{1/2}$ and Z were determined by fitting G-V curves to a Boltzmann function ($G=G_{max}[1/(1+e^{-(V-V1/2)ZF/RT)}]$) and then by normalizing to the maximum of the fit.

qPCR

Total RNA was isolated from hippocampi of 3 WT and 3 β4KO age-matched animals at concentration of about 30 ng/μl. RNA was reverse-transcribed into cDNA with random primers. RT-qPCR was carried out using ABI Prism 7900 HT detection system and Power SYBR Green master mix (Applied Biosystems, Carlsbad, CA, USA). qPCR specificity was checked by dissociation curve analysis. Reaction volumes of 50 μl were used with 1 μl of template cDNA and 5 μl of 10x primers. Specific primers were purchased from a commercial vendor (Qiagen, Valencia, CA, USA) based on published sequences (Yang *et al.*, 2009). Reactions were run in triplicates for each individual brain cDNA. Amplification conditions consisted of 10 minutes denaturation at 95°C followed by 40 cycles of 95°C denaturation for 15 seconds and 60°C annealing and elongation. The results were analyzed using SDS2.1.1 software (Applied Biosystems, Carlsbad, CA, USA) following the $2^{-\Delta\Delta CT}$ method and normalized by the expression levels of the housekeeping gene, Gapdh, which was quantified for each individual brain cDNA in triplicates. Significant differences were assessed using the unpaired, one-tailed Student's t-test and the Excel software (Microsoft).

RESULTS

Fostriecin reduces action potential amplitudes of β4 knockout but not wild type neurons

To investigate the role of PP2A/PP4 in modulating BK channel-dependent changes in excitability, we measured action potential shape and firing properties of neurons from wild type (WT) and β4 knockout (KO) mice. We recorded from dentate gyrus granule neurons where both the BK channel pore-forming α and β4 accessory subunits are expressed (Brenner *et al.*, 2005; Petrik & Brenner, 2007). The PP2A/PP4-specific blocker Fostriecin was applied into the cell via the recording pipette to inhibit phosphatase activity, and BK-channel specific effects were evaluated by application of the BK channel-specific blocker Paxilline.

Figure 1 shows representative action potentials (10^{th} AP of a spike train) during a 210 pA current injection that are aligned to the threshold voltage for comparison. For WT neurons, Fostriecin inhibition of PP2A/PP4 shows no significant effect on the action potential waveform with regard to amplitude, width or fast afterhyperpolarization (fAHP) amplitude (Fig. 1A WT trace, 1B–1D summary data). Further block with Paxilline shows no effect (Figure 1A, WT trace), consistent with previous studies that the β4 subunit reduces recruitment of BK channels during action potentials (Brenner *et al.*, 2005). In β4 KO however, PP2A/PP4 inhibition dramatically reduces peak amplitude by 17 mV, from a control value of 80 ± 4.0 mV to 63.7 ± 7.5 mV after Fostriecin ($P = 0.038$ unpaired t-test, df = 17, Fig. 1A, 1B). The truncation of action potential amplitude is due to a reduction of the peak, not changes in threshold since the interspike voltages are the same between controls and Fostriecin treated cells (for example, interspike voltages elicited by 210 pA current injections in KO neurons are −36.7 ± 2.9 mV for control, −37.9 ± 1.2 mV for Fostriecin, −38.6 ± 1.1 mV for Fostriecin/Paxilline, n = 10, 9 and 12, respectively, $P > 0.35$, unpaired t-test). The effect of PP2A/PP4 inhibition on action potentials is likely to be BK channel-specific since Paxilline inhibition of BK channels reverses these effects (Fig. 1A, right panel, Fig. 1B, right bar graphs), and Paxilline does not truncate action potentials in the absence of Fostriecin (Brenner *et al.*, 2005). Further, the observation that BK channel block

prevents Fostriecin truncation of the action potential suggests that PP2A/PP4 inhibition acts to increase BK channel current during the action potential. Consistent with this, β4 inhibition of BK channels in WT neurons prevents Fostriecin effects on action potential amplitude.

Secondary effects on the action potential waveform accompany the reduction of the action potential amplitude in KO neurons. The action potential width is broadened ($P = 0.047$ unpaired t-test, df = 18, KO control 1.53 ± 0.06 ms, versus KO with Fostriecin, 2.0 ± 0.24 ms, Fig. 1C) and the AHP is reduced ($P = 0.01$ unpaired t-test, df = 18, KO control −9.9 ± 0.43 mV, versus KO with Fostriecin, −7.4 ± 0.88 ms, Fig. 1D). This may be due to reduced activation of delayed rectifier potassium current that accompanies a shorter action potential. BK channel truncation of action potentials has been shown previously to reduce delayed rectifier potassium current recruitment in anterior pituitary neurons (Van Goor *et al.*, 2001).

Inhibition of PP2A/PP4 increases excitability of neurons

Inhibition of PP2A/PP4 increases firing rates in both WT and KO neurons (Fig. 2A, 2B). In a number of preparations, BK channel block reduces action potential frequency (Brenner *et al.*, 2005; Gu *et al.*, 2007; Shruti *et al.*, 2008). BK channel block with Paxilline however only partially reversed Fostriecin effects on firing rate in DG neurons (Fig 2B). This suggests that PP2A/PP4 inhibition has effects on firing that are in addition to those on BK channels. BK channel-specific effects are nevertheless discerned when analyzing instantaneous action potential frequency that is more reflective of the interspike-intervals during the action potential train (Fig. 2D, 2E). The results show that BK channel block significantly attenuates the Fostriecin mediated decrease in interspike intervals in KO during the early spikes of the action potential train (Fig. 2E). In WT neurons, Paxilline tends to moderate firing but this does not reach statistical significance ($P > 0.1$, df = 13, unpaired t-test, Fig. 2D).

We also observed an effect of Fostriecin on DG neuronal excitability that is not dependent on BK channels since they are not reversed by Paxilline block. This is a negative voltage shift of action potential thresholds elicited by ramped current injections. Action potential thresholds tended to be shifted by an approximate −7 and −12 mV for WT and KO neurons, respectively (WT from −33.6 ± 4.3 mV to −40.9 ± 1.9 mV with Fostriecin, $P = 0.07$, df = 16, KO from −24.4 ± 5.1 mV to −36.3 ± 2.7 mV with Fostriecin, $P = 0.03$, df = 17, unpaired t-test, see Table 1). The affect on action potential threshold appears to be specific to ramped current injections approaching threshold, but not during a square-wave current injection or during an ensuing action potentials train. As discussed above, Fostriecin does not alter interspike voltages during square wave (210 pA) current injections. This suggests that Fostriecin may affect subthreshold currents that are otherwise not active, or are a smaller fraction of the total permeability, during action potential trains.

In conclusion, these results suggest that BK channel activation is required for several effects of PP2A/PP4 blocker Fostriecin. These include truncation of action potentials and increase of early spiking instantaneous frequency. An important role for the β4 subunits, therefore, is to oppose all of the above effects by reducing BK channel opening.

Block of PP2A/PP4 increases BK current in neurons but not in isolated BK channels

The results from brain slice recordings suggest that blocking PP2A/PP4 in neurons activates BK channels. We therefore used voltage clamp recordings to test if Fostriecin increases BK currents in dentate gyrus neurons. We measured BK currents from the β4 KO granule neurons using paired recordings to isolate Paxilline-sensitive currents in control (Fig. 3A) and Fostriecin treated neurons (Fig. 3B). Results for BK currents are summarized as current

density as a function of voltage (Fig. 3C). Current density for BK currents treated with Fostriecin is larger than controls. Over a wide range of voltages, Fostriecin almost doubles the current density of BK channels. For example, at +30 mV the BK current density increases from 17.6 ± 8.5 pA/pF to 39.7 ± 4.5 pA/pF (P = 0.02, df = 12, unpaired t-test). In addition to an increase of BK current, Fostriecin causes a speeding of BK current activation kinetics to submillisecond times (Fig. 3D, (P = 0.04 at +60 mV, df = 12, unpaired t-test)). The faster activation in β4 KO may explain the ability of BK channels to truncate action potential peaks (Fig. 1).

PP2A is expressed in many cell types including the dentate gyrus of the hippocampus (Vogelsberg-Ragaglia *et al.*, 2001), but also in cell lines like HEK293 cells (Lechward *et al.*, 2006). The results from brain slice recordings suggest that blocking PP2A/PP4 in the β4 KO neurons increases BK currents to alter neuronal excitability. However it is not clear whether these effects are direct or indirect actions on BK channels. We therefore expressed BK channels in HEK293 cells and measured their response to the PP2A/PP4 inhibitor. Unlike DG neurons, we found that Fostriecin failed to activate BK channels in HEK 293 cells (supplement Fig. 1). Half-maximal voltage dependence of activation ($V_{1/2}$) showed no significant difference with Fostriecin (59.6 ± 2.4 mV without versus 63.0 ± 5.8 mV with Fostriecin, supplement Fig. 1B, P = 0.3, df = 17, unpaired t-test). Nor was activation kinetics significantly increased (4.8 ± 0.8 ms control versus 6.2 ± 0.8 ms activation tau with Fostriecin at +80 mV, P = 0.13, df = 21, unpaired t-test). To confirm that PP2A/PP4 was present to modulate BK channels in this preparation, we examined the effect of transfected α + β4 BK channels in HEK293 cells. Previous studies suggest that type II BK channels, which are likely to be composed of α+ β4 subunits, are activated by PP2A (Reinhart *et al.*, 1991). Consistent with PP2A activation of α+ β4 subunits, we saw that PP2A inhibitor Fostriecin inhibited α+ β4 BK currents. Fostriecin caused a 13 mV positive shift in the conductance-voltage relationship (P = 0.027 at $V_{1/2}$, df = 19, unpaired t-test, supplement Fig. 1D) indicating that PP2A/PP4 is available to modulate BK channels given co-expression of the accessory subunit.

The lack of effect on isolated α alone BK channels (HEK293 cells) compared to BK current activation by PP2A/PP4 inhibition in neurons may be explained by activation of voltage-gated calcium currents that secondarily activate BK channels in neurons. Therefore, we wished to determine effects of PP2A/PP4 inhibition on voltage-gated calcium currents from the dentate gyrus granule neuron. It is possible that calcium current recordings of dentate gyrus neurons in brain slices suffer from incomplete voltage clamp due to their dendritic trees (Rahimi & Claiborne, 2007). Nevertheless, we attempted to discern a difference in calcium current due to PP2A/PP4 inhibition and discarded currents that show extensive space clamp problems. We used ionic solutions and select channel inhibitors (see Methods) to ensure > 95 % of the current is calcium channel specific (as evidenced by cadmium block, see supplement Fig. 2). As previously shown, total calcium currents from dentate granule neurons have a very steep voltage activation that peaks at −20 mV (Blaxter *et al.*, 1989). There indeed was an increase in the calcium currents in Fostriecin-treated neurons (Fig. 4B) when compared with control (Fig. 4A). For example, at −20 mV the current density increases from control −98 ± 20 pA/pF to −192± 34 pA/pF in Fostriecin-treated neurons (P = 0.02, df = 11, unpaired t-test, Fig. 4C). At more positive voltages, such as +10 mV, Fostriecin increases granule cell current density from −25 ± 7 A/pF to −54 ± 12 pA/pF (P = 0.025, df = 11, unpaired t-test, Fig. 4C).

Utilizing the non-specific calcium channel blocker, cadmium (200 μM), we tested whether Fostriecin truncation of action potentials are dependent on calcium influx. Figure 6 shows action potentials of KO treated cells with cadmium alone, or with cadmium and Fostriecin. Cadmium alone appears to depolarize baseline voltage perhaps through inhibition of

calcium-activated currents (baseline voltage is −36.7 ± 2.9 mV for KO, −18 ± 3.5 mV for KO + cadmium, −20 ± 2.5 mV for KO + cadmium and Fostriecin, $P < 0.001$ unpaired t-test for control versus cadmium treated, df = 18, or control versus cadmium/Fostriecin treated, df = 20). Nevertheless, Fostriecin does not further truncate action potentials in the presence of cadmium (Fig. 5A and 5B). As well, Fostriecin lacks other effects that are otherwise observed in the absence of cadmium such as broadening of the half-width (Fig. 5C), reduction of the fAHP (Fig. 5D), and increases of frequency (Fig. 5E and 5F) ($P > 0.2$ for all data, unpaired t-test, df = 18 for all data).

Finally, there is a possibility that the observed effects of Fostriecin in the β4 KO granule cells are a result of altered expression of the other β subunits as the consequence of the knocking-out of the β4 subunit. We therefore compared the relative expression levels of the β subunits, mSlo1 and mSlo3 genes from total RNA isolated from the hippocampi of WT and β4 KO animals. Our RT-qPCR results (supplement Fig. 2B) show no difference in expression of mSlo1, mSlo3 and β1, β2 and β3 subunits between the WT and β4 KO animals. However, the results confirm a dramatic, four orders of magnitude reduction of the β4 subunit expression in the β4 KO versus WT animals confirming the knock-out genotype.

Although we cannot exclude the possibility that PP2A/PP4 dephosphorylates BK channels directly in neurons but not HEK293 cells, these results correlate increased BK channel currents by PP2A/PP4 inhibition with an increase of calcium currents. Furthermore, the presence of the inhibitory β4 subunit in WT neurons prevents many functional consequences of BK channel activation by PP2A/PP4 inhibition.

cAMP-dependent phosphorylation mimics effects of Fostriecin on AP amplitude

In a number of studies, $CaV_{1.2}$ L-type voltage-dependent calcium channels are activated by cAMP-dependent protein kinase and this effect is opposed by PP2A at the same phosphorylation site (Davare *et al.*, 2000); (Hall *et al.*, 2006). Given that $CaV_{1.2}$ channels are expressed in dentate gyrus granule cells (Tippens *et al.*, 2008), we tested the possibility that cAMP could replicate some effects of PP2A/PP4 inhibition. We subjected the granule cells to 1 mM cAMP in the intracellular solution while using the whole cell configuration. The aim was to activate PKA in the presence or absence of Paxilline and see if it can achieve similar effects on action potential waveforms as protein phosphatase inhibition.

In KO neurons cAMP replicated effects of Fostriecin with regard to action potential amplitude and width (Fig. 6A–6C). cAMP leads to truncated action potential amplitude (from 80 ± 4 mV for control to 62 ± 6 mV after cAMP, $P = 0.013$, df = 16, unpaired t-test, Fig. 6A–B). Half-width is increased from 1.5 ± 0.1 ms in control to 2.4 ± 0.4 ms after cAMP ($P = 0.026$, df = 16, unpaired t-test, Fig. 6C). Both effects are reversed by co-application of Paxilline, indicating that these are BK channel-specific. Although fAHP amplitude was also reduced by cAMP (Fig. 6D), this effect was only partially reversed by Paxilline suggesting some BK channel-independent effects on this property. In WT neurons activation of PKA did not significantly alter action potential amplitude or half-width (Fig. 6A–C). Unlike Fostriecin, there however was a reduction of the fAHP that was not dependent on BK channels since co-application of Paxilline did not reverse these effects (Fig. 6D). In summary, we find that the protein kinase A activator, cAMP, similarly affects action potential amplitude as the PP2A/PP4 inhibitor Fostriecin. These effects are not seen in the presence of BK channel inhibition with the β4 subunit (wild type) or by BK channel block with Paxilline. cAMP also reduces the fAHP (Fig. 6D) in both WT and KO in a manner that is BK channel-independent.

DISCUSSION

Neurons utilize a rich assortment of ion channels to tailor their electrical properties. Phosphorylation-dependent changes of ion channel gating provide the neurons with the ability to dynamically alter their membrane excitability. In this study, we investigated phosphorylation-dependent changes in the excitability of the hippocampal granule cells due to BK channels. To discern BK channel-specific effects, we identified changes that were reversed with the BK channel blocker Paxilline. We also compared changes with and without the BK channel inhibitory β4 subunit utilizing knockout mice in order to elucidate how the neuron-specific accessory subunit affects responsiveness of BK channels to phosphorylation. By these criteria, we identified two major effects that could be attributable to BK channel modulation by the phosphorylation status of the neurons. These were a truncation of the action potential amplitude and an increase in spike frequency during the early components of an action potential train. These effects were observed only in the absence of the β4 subunit suggesting its novel role as a factor that prevents over-activation of BK channels by cellular phosphorylation.

How does Paxilline oppose Fostriecin effects? The most likely interpretations for Paxilline-dependency of these effects is that phosphatase inhibition directly or indirectly (through voltage-dependent calcium channels), activate BK channels. Therefore Paxilline block occludes these effects. An alternative argument may be that BK channels and phosphatase inhibition are independent but share similar effects. Therefore, Paxilline block of BK channels would appear to oppose Fostriecin effects. Supporting the former argument (that BK channels are downstream of Fostriecin actions) is our previous study showing that Paxilline or β4 do not reduce action potential amplitude or promote spike failures in the absence of Fostriecin (Brenner *et al.*, 2005). An exception is the Paxilline reduction of firing rates that is also seen in the absence of PP2A/PP4 inhibition (Brenner *et al.*, 2005), and therefore it is not certain whether effects on instantaneous firing rates are downstream of Fostriecin.

Traditionally, BK channels are implicated in the repolarization and fast afterhyperpolarization phases of the action potential waveform (Storm, 1987; Lovell & McCobb, 2001); (Faber & Sah, 2002; Brenner *et al.*, 2005; Gu *et al.*, 2007). Our novel finding that BK channels in DG neurons can also reduce the action potential amplitude is somewhat unusual but has a precedent in pituitary somatotrophs (Van Goor *et al.*, 2001). In these cells, BK channel truncation of action potentials reduces activation of delayed rectifier potassium current that prolongs action potential bursts (Van Goor *et al.*, 2001). Similarly, in the DG granule neurons BK channel truncation of action potentials appears to secondarily broaden action potentials, perhaps due to reduced delayed rectifier current. Our results show that truncation of action potentials is mediated by PP2A/PP4 inhibition that activates BK channels. We did not observe a change in resting voltage, inter-spike voltage or AHP that would account for Fostriecin reduction of action potential amplitude. Instead, BK channels are likely to be activated in the depolarization phase that, combined with an increased potassium driving force during the action potential, may truncate the action potential. This would require relatively fast BK channel activation kinetics, consistent with fast-gated type I BK channels or BK channels lacking the β4 subunit (Reinhart *et al.*, 1989; Wang *et al.*, 2009). Indeed, Fostriecin-induced truncation of action potentials was correlated with BK channel speeding of activation kinetics and increase of current, and increased of voltage-dependent calcium current; all of which would contribute to BK channel activation during the action potential. On the other hand, although Fostriecin causes a positive G-V shift of α+β4 BK channels in HEK 293 cells, this effect did not result in an increase of action potential amplitudes in wild type DG neurons. Nor did indirect Fostriecin effects on voltage-dependent calcium channels alter wild type action potential amplitude. Thus, one may

surmise that the slow gating conferred by the β4 subunit (Brenner et al., 2000b; Brenner et al., 2005; Wang et al., 2009) may prevent BK channel recruitment and regulation of action potential shape, despite Fostriecin direct and indirect affects on channel opening.

We observed a similar BK-dependent truncation of action potential amplitude with application of cAMP as phosphatase inhibitor. This suggests that reduction in PP2A/PP4 dephosphorylation leads to increased PKA-dependent phosphorylation. A similar phenomenon was shown previously in BK channels from an anterior pituitary cell line (Tian *et al.*, 1998). The fact that we observed these effects only in the β4 KO neurons suggest that knockout of the β4 subunit unmasks BK channel effects on action potential amplitude following changes in phosphorylation state. In other words, the β4 subunit protects the BK channels against the overactivation that may arise from dramatic changes in the phosphorylation status of the cell.

The most parsimonious conclusion from this study is that Fostriecin effects are BK channel-dependent but indirect through activation of calcium channels. This conclusion is supported by the fact that Fostriecin does not activate isolated BK channels in HEK293 cells, but does activate both BK and voltage-dependent calcium channels in neurons. This is also supported by previous findings that PP2A directly attaches to $CaV_{1.2}$ L-type calcium channels and antagonizes PKA activation channels through a common phosphorylation site (Davare *et al.*, 2000; Hall *et al.*, 2006). Indeed, the fact that BK channels are physically coupled to $CaV_{1.2}$ channels in neurons (Berkefeld *et al.*, 2006) and that cAMP confers similar effects on action potential amplitude as Fostriecin, supports such a model.

In a broader sense, these findings also suggest that BK and calcium channels should not be considered in isolation, as modulation of one channel may have dramatic affects on the other. Calcium channels are modulated by a number of phosphorylation-dependent and independent second messengers (Felix, 2005). Common observations of BK-CaV functional coupling (Marrion & Tavalin, 1998; Prakriya & Lingle, 1999; 2000; Sun *et al.*, 2003), which has been confirmed by demonstration of physical coupling (Berkefeld *et al.*, 2006) suggest that functional outcomes of CaV channel modulations needs to be considered in light of their potential effects on BK channels.

Supplementary Material

Refer to Web version on PubMed Central for supplementary material.

Acknowledgments

We acknowledge Luke Whitmire for critical reading of this manuscript. This work was supported by a NIH NINDS grant (NS052574) to Robert Brenner, and AHA grant BGIA 2390030 to Bin Wang.

References

Behrens R, Nolting A, Reimann F, Schwarz M, Waldschutz R, Pongs O. hKCNMB3 and hKCNMB4, cloning and characterization of two members of the large-conductance calcium-activated potassium channel beta subunit family. FEBS Lett. 2000; 474:99–106. [PubMed: 10828459]

Berkefeld H, Sailer CA, Bildl W, Rohde V, Thumfart JO, Eble S, Klugbauer N, Reisinger E, Bischofberger J, Oliver D, Knaus HG, Schulte U, Fakler B. BKCa-Cav channel complexes mediate rapid and localized Ca2+-activated K+ signaling. Science. 2006; 314:615–620. [PubMed: 17068255]

Blaxter TJ, Carlen PL, Niesen C. Pharmacological and anatomical separation of calcium currents in rat dentate granule neurones in vitro. J Physiol. 1989; 412:93–112. [PubMed: 2557433]

Brenner R, Chen QH, Vilaythong A, Toney GM, Noebels JL, Aldrich RW. BK channel beta4 subunit reduces dentate gyrus excitability and protects against temporal lobe seizures. Nat Neurosci. 2005; 8:1752–1759. [PubMed: 16261134]

Brenner R, Jegla TJ, Wickenden A, Liu Y, Aldrich RW. Cloning and functional characterization of novel large conductance calcium-activated potassium channel beta subunits, hKCNMB3 and hKCNMB4. J Biol Chem. 2000a; 275:6453–6461. [PubMed: 10692449]

Brenner R, Perez GJ, Bonev AD, Eckman DM, Kosek JC, Wiler SW, Patterson AJ, Nelson MT, Aldrich RW. Vasoregulation by the beta1 subunit of the calcium-activated potassium channel. Nature. 2000b; 407:870–876. [PubMed: 11057658]

Cui J, Cox DH, Aldrich RW. Intrinsic voltage dependence and Ca2+ regulation of mslo large conductance Ca-activated K+ channels. J Gen Physiol. 1997; 109:647–673. [PubMed: 9154910]

Davare MA, Horne MC, Hell JW. Protein phosphatase 2A is associated with class C L-type calcium channels (Cav1.2) and antagonizes channel phosphorylation by cAMP-dependent protein kinase. J Biol Chem. 2000; 275:39710–39717. [PubMed: 10984483]

Faber ES, Sah P. Physiological role of calcium-activated potassium currents in the rat lateral amygdala. J Neurosci. 2002; 22:1618–1628. [PubMed: 11880492]

Felix R. Molecular regulation of voltage-gated Ca2+ channels. J Recept Signal Transduct Res. 2005; 25:57–71. [PubMed: 16149767]

Gu N, Vervaeke K, Storm JF. BK potassium channels facilitate high-frequency firing and cause early spike frequency adaptation in rat CA1 hippocampal pyramidal cells. J Physiol. 2007; 580:859–882. [PubMed: 17303637]

Ha TS, Heo MS, Park CS. Functional effects of auxiliary beta4-subunit on rat large-conductance Ca(2+)-activated K(+) channel. Biophys J. 2004; 86:2871–2882. [PubMed: 15111404]

Hall DD, Feekes JA, Arachchige Don AS, Shi M, Hamid J, Chen L, Strack S, Zamponi GW, Horne MC, Hell JW. Binding of protein phosphatase 2A to the L-type calcium channel Cav1.2 next to Ser1928, its main PKA site, is critical for Ser1928 dephosphorylation. Biochemistry. 2006; 45:3448–3459. [PubMed: 16519540]

Horrigan FT, Aldrich RW. Coupling between voltage sensor activation, Ca2+ binding and channel opening in large conductance (BK) potassium channels. J Gen Physiol. 2002; 120:267–305. [PubMed: 12198087]

Lechward K, Sugajska E, de Baere I, Goris J, Hemmings BA, Zolnierowicz S. Interaction of nucleoredoxin with protein phosphatase 2A. FEBS Lett. 2006; 580:3631–3637. [PubMed: 16764867]

Lewy DS, Gauss CM, Soenen DR, Boger DL. Fostriecin: chemistry and biology. Curr Med Chem. 2002; 9:2005–2032. [PubMed: 12369868]

Lovell PV, McCobb DP. Pituitary control of BK potassium channel function and intrinsic firing properties of adrenal chromaffin cells. J Neurosci. 2001; 21:3429–3442. [PubMed: 11331373]

Marrion NV, Tavalin SJ. Selective activation of Ca2+-activated K+ channels by co-localized Ca2+ channels in hippocampal neurons. Nature. 1998; 395:900–905. [PubMed: 9804423]

Martin GE, Hendrickson LM, Penta KL, Friesen RM, Pietrzykowski AZ, Tapper AR, Treistman SN. Identification of a BK channel auxiliary protein controlling molecular and behavioral tolerance to alcohol. Proc Natl Acad Sci U S A. 2008

Meera P, Wallner M, Toro L. A neuronal beta subunit (KCNMB4) makes the large conductance, voltage- and Ca2+-activated K+ channel resistant to charybdotoxin and iberiotoxin. Proc Natl Acad Sci U S A. 2000; 97:5562–5567. [PubMed: 10792058]

Orio P, Rojas P, Ferreira G, Latorre R. New disguises for an old channel: MaxiK channel beta-subunits. News Physiol Sci. 2002; 17:156–161. [PubMed: 12136044]

Petrik D, Brenner R. Regulation of STREX exon large conductance, calcium-activated potassium channels by the beta4 accessory subunit. Neuroscience. 2007; 149:789–803. [PubMed: 17945424]

Prakriya M, Lingle CJ. BK channel activation by brief depolarizations requires Ca2+ influx through L- and Q-type Ca2+ channels in rat chromaffin cells. J Neurophysiol. 1999; 81:2267–2278. [PubMed: 10322065]

Prakriya M, Lingle CJ. Activation of BK channels in rat chromaffin cells requires summation of Ca(2+) influx from multiple Ca(2+) channels. J Neurophysiol. 2000; 84:1123–1135. [PubMed: 10979988]

Rahimi O, Claiborne BJ. Morphological development and maturation of granule neuron dendrites in the rat dentate gyrus. Prog Brain Res. 2007; 163:167–181. [PubMed: 17765718]

Reinhart PH, Chung S, Levitan IB. A family of calcium-dependent potassium channels from rat brain. Neuron. 1989; 2:1031–1041. [PubMed: 2624739]

Reinhart PH, Chung S, Martin BL, Brautigan DL, Levitan IB. Modulation of calcium-activated potassium channels from rat brain by protein kinase A and phosphatase 2A. J Neurosci. 1991; 11:1627–1635. [PubMed: 1646298]

Sah P, Faber ES. Channels underlying neuronal calcium-activated potassium currents. Prog Neurobiol. 2002; 66:345–353. [PubMed: 12015199]

Shruti S, Clem RL, Barth AL. A seizure-induced gain-of-function in BK channels is associated with elevated firing activity in neocortical pyramidal neurons. Neurobiol Dis. 2008; 30:323–330. [PubMed: 18387812]

Storm JF. Intracellular injection of a Ca2+ chelator inhibits spike repolarization in hippocampal neurons. Brain Res. 1987; 435:387–392. [PubMed: 3123013]

Sun X, Gu XQ, Haddad GG. Calcium influx via L- and N-type calcium channels activates a transient large-conductance Ca2+-activated K+ current in mouse neocortical pyramidal neurons. J Neurosci. 2003; 23:3639–3648. [PubMed: 12736335]

Tian L, Knaus HG, Shipston MJ. Glucocorticoid regulation of calcium-activated potassium channels mediated by serine/threonine protein phosphatase. J Biol Chem. 1998; 273:13531–13536. [PubMed: 9593688]

Tippens AL, Pare JF, Langwieser N, Moosmang S, Milner TA, Smith Y, Lee A. Ultrastructural evidence for pre- and postsynaptic localization of Cav1.2 L-type Ca2+ channels in the rat hippocampus. J Comp Neurol. 2008; 506:569–583. [PubMed: 18067152]

Van Goor F, Li YX, Stojilkovic SS. Paradoxical role of large-conductance calcium-activated K+ (BK) channels in controlling action potential-driven Ca2+ entry in anterior pituitary cells. J Neurosci. 2001; 21:5902–5915. [PubMed: 11487613]

Vogelsberg-Ragaglia V, Schuck T, Trojanowski JQ, Lee VM. PP2A mRNA expression is quantitatively decreased in Alzheimer's disease hippocampus. Exp Neurol. 2001; 168:402–412. [PubMed: 11259128]

Wang B, Rothberg BS, Brenner R. Mechanism of increased BK channel activation from a channel mutation that causes epilepsy. J Gen Physiol. 2009; 133:283–294. [PubMed: 19204188]

Weiger TM, Holmqvist MH, Levitan IB, Clark FT, Sprague S, Huang WJ, Ge P, Wang C, Lawson D, Jurman ME, Glucksmann MA, Silos-Santiago I, DiStefano PS, Curtis R. A novel nervous system beta subunit that downregulates human large conductance calcium-dependent potassium channels. J Neurosci. 2000; 20:3563–3570. [PubMed: 10804197]

Yang CT, Zeng XH, Xia XM, Lingle CJ. Interactions between beta subunits of the KCNMB family and Slo3: beta4 selectively modulates Slo3 expression and function. PLoS One. 2009; 4:e6135. [PubMed: 19578543]

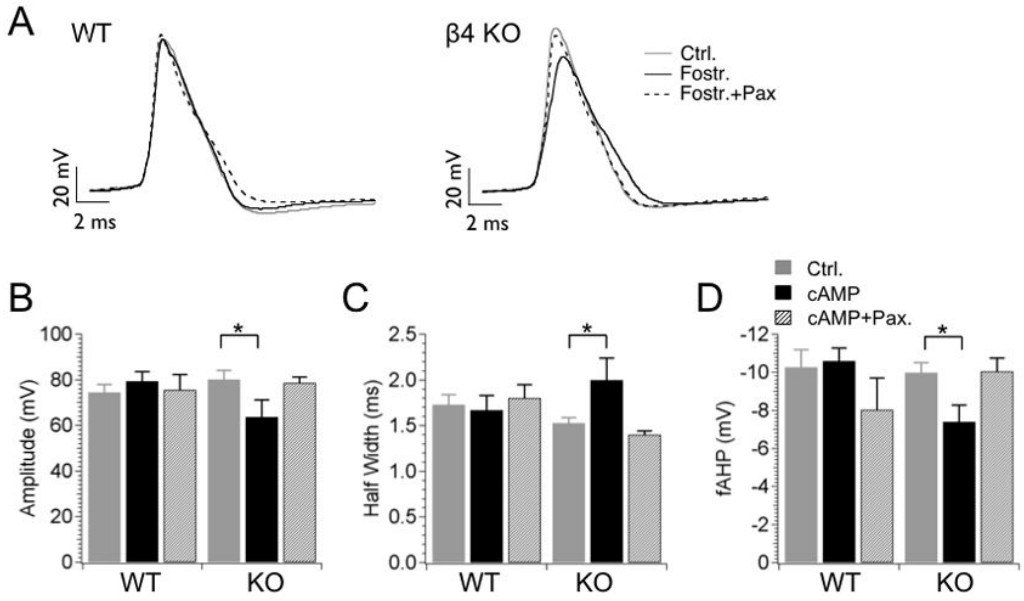

Figure 1. Protein phosphatase inhibition reduces action potential amplitudes in β4 knockout neurons

(A) Example action potential waveforms recorded from WT and β4 KO neurons during 210 pA current injection. Representative 10th action potentials from an action potential train of control neurons (solid gray line), neurons treated with 250 nM Fostriecin (solid dark line), and neurons treated with Fostriecin and 5 μM Paxilline (dashed line). (B–D) Plots of averaged action potential properties including action potential amplitude (B), half-width (C) and fAHP amplitude (D). First columns represent control; second columns are for Fostriecin application (intracellular), third columns are for Fostriecin (intracellular) with Paxilline in the bath.

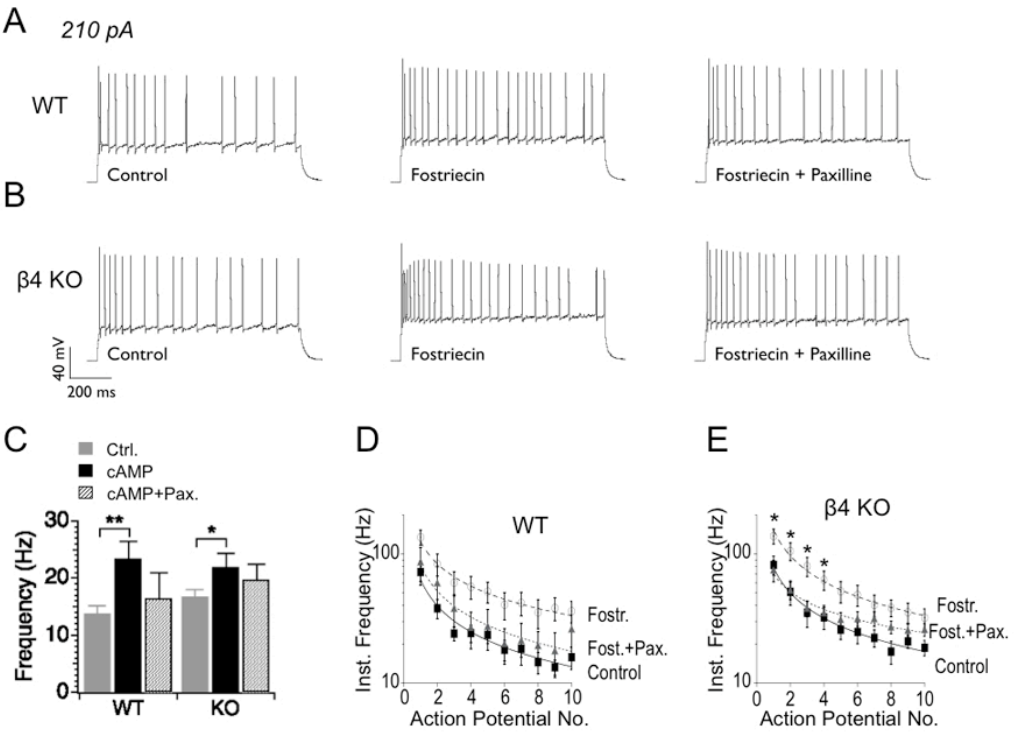

Figure 2. Fostriecin block of phosphatase activity causes BK channel-dependent increases in instantaneous firing frequency

(A, B) Examples of action potential trains elicited by 210 pA current injection for WT and KO neurons, respectively. Traces from control (left) are compared with traces recorded after application of Fostriecin alone (middle) or Fostriecin with Paxilline (right). (C) Summarized firing frequency from a one second current (210 pA) injection in WT and β4 KO neurons, respectively. (D, E) Instantaneous firing frequency is for the first ten action potentials during a 210 pA current injection.

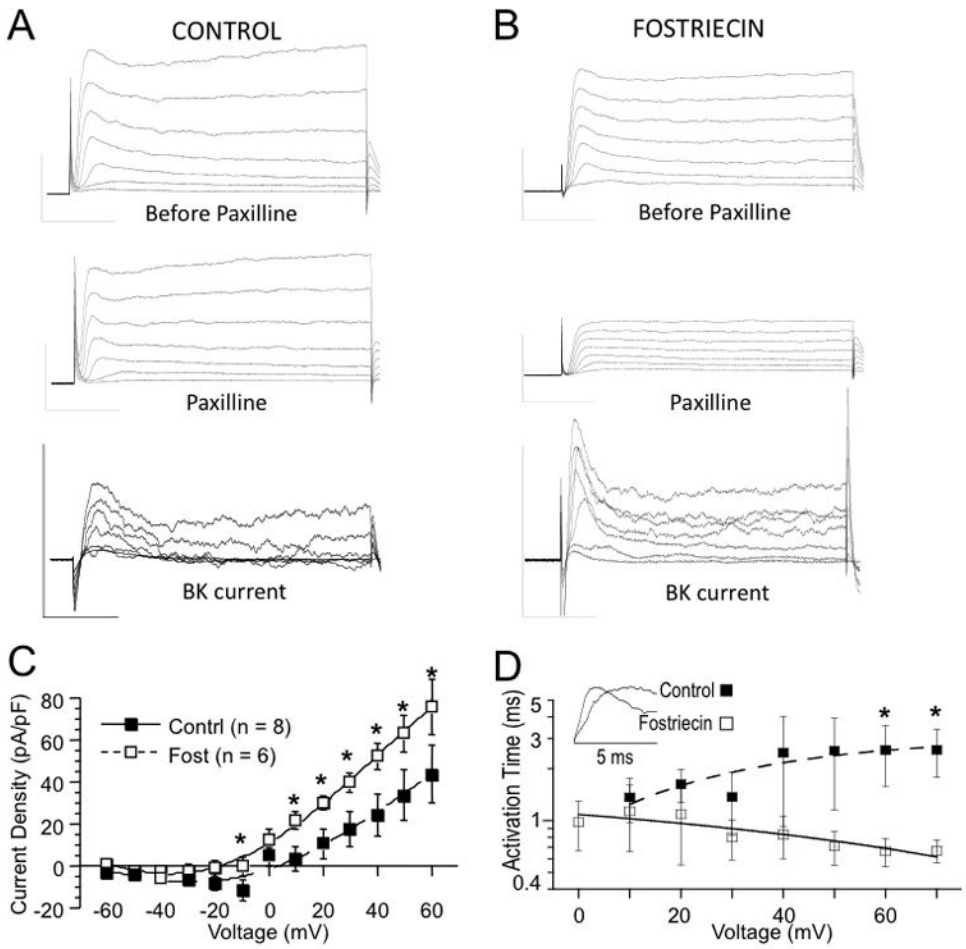

Figure 3. Fostriecin block of phosphatase activity increases BK currents in β4 KO neurons

(A) Example traces before (upper panel) and 10 minutes after application of BK channel blocker Paxilline (middle panel). Lower panel shows subtracted net BK current. (B) Example isolation of BK current from a Fostriecin treated cell. Vertical scale represents 1 nA current (vertical) and 10 ms time (horizontal). (C) Current density is summarized for BK current as a function of voltage. Filled symbols are for control, empty symbols are for Fostriecin-treated cells. Numbers in parentheses represent number of measured cells. (D) Activation time of isolated BK current is shorter with Fostriecin treatment. Inset shows example isolated BK current traces during first 5 millisecond of a +60 mV voltage step.

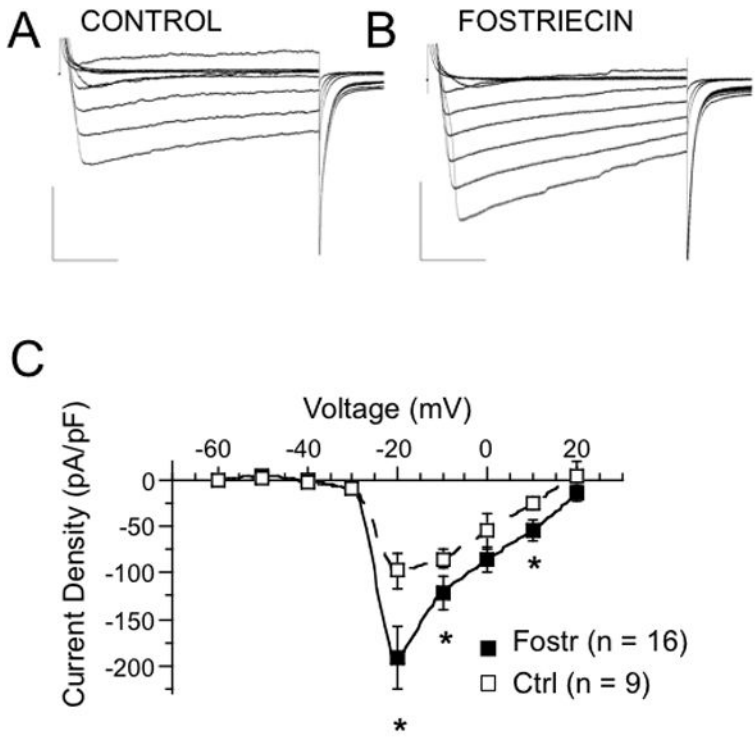

Figure 4. Fostriecin block of phosphatase activity increases voltage-dependent calcium currents in the granule neurons of the β4 KO mice

Representative whole-cell currents from control (A) and from a cell treated with intracellular 250 nM Fostriecin (B) are summarized as current density as a function of command voltage (C). Traces shown are in 20 mV intervals from −60 mV to +60 mV. The numbers in parentheses represent number of measured cells. All measurements were done in the presence of blockers of voltage-dependent potassium and sodium currents (see Methods). An interpolation was used to connect the data points.

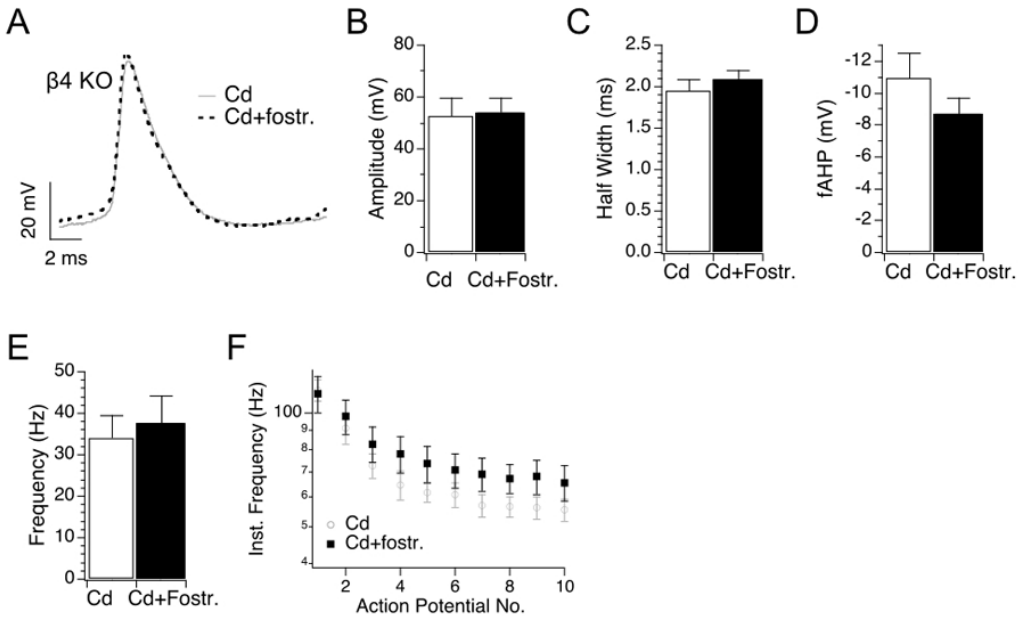

Figure 5. Cadmium block of calcium influx occludes effects of protein phosphatase inhibition

(A) Example β4 KO action potential waveforms recorded in cadmium alone (200 μM cadmium, grey line) or cadmium with Fostriecin (dashed line). Representative 10th action potentials from an action potential train during 210 pA current injection. (B-D) Plots of averaged action potential properties including action potential amplitude (B), half-width (C), fAHP amplitude (D), frequency (E) and instantaneous frequency (F).

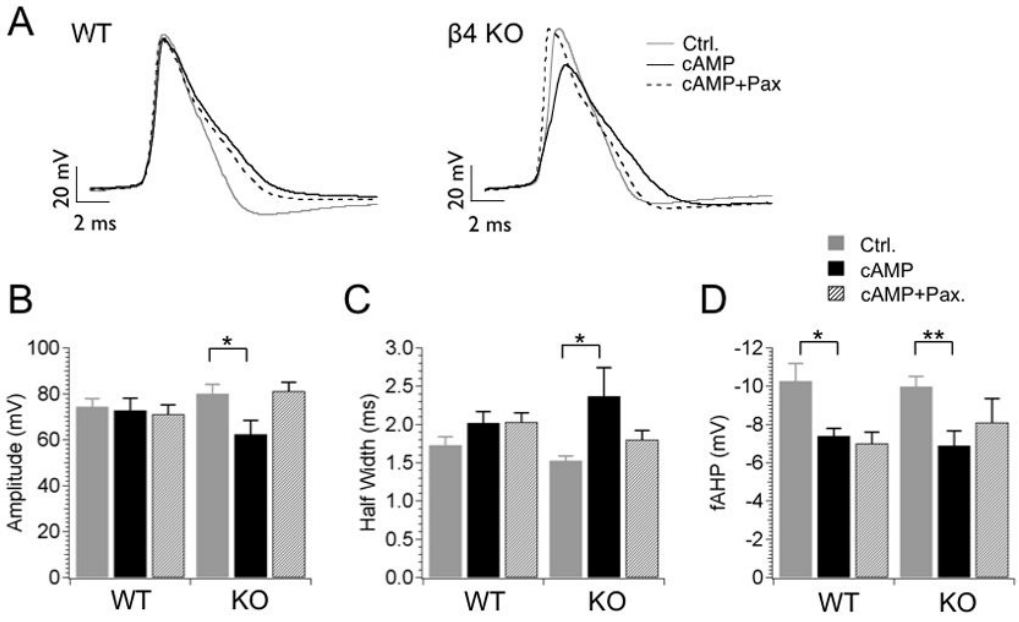

Figure 6. cAMP reproduces effects of Fostriecin on action potential amplitude and half-width in KO neurons

(A) Example action potential waveforms recorded from WT and β4 KO neurons during 210 pA current injection. The plots represent 10th action potentials from action potential trains of control (un-treated) neurons (solid gray line) and from neurons treated with 1 mM intracellular cAMP (solid dark line). Co-application of BK channel specific blocker 5 μM Paxilline with cAMP (dashed line) is also shown. Scale bars are 20 mV (for voltage axis) and 2 ms (for time axis). (B–D) Plots show averaged action potential properties including action potential amplitude (B), half-width (C) and fAHP amplitude (D). Data are shown for the 10th action potential during a 210 pA current injection. Taken from left, first columns represent control, second (middle) columns are for cAMP in the pipette (intracellular), third columns are for cAMP (pipette) and Paxilline in the bath solution.

Table 1

Intrinsic membrane properties in dentate gyrus granule neurons in response to Fostriecin and cAMP

RMP, resting membrane potential, IR, input resistance, Threshold, action potential threshold during a 125 pA ramped current injection.

Treatment	Background	RMP (mV)	IR (MΩ)	Threshold (mV)
Control	WT	−86.8±1.1	547±61	−33.6±4.3
	β4 KO	−86.3±0.9	557±60	−24.4±5.1
Fostriecin	WT	−86.1±0.9	593±98	−40.9±1.9
	β4 KO	−85.0±0.8	626±59	−36.3±2.7
Fostriecin+Pax.	WT	−84.2±1.2	568±84	−39.6±3.1
	β4 KO	−85.4±0.9	508±41	−37.5±1.3
cAMP	WT	−83.7±1.0	491±76	−37.8±1.3
	β4 KO	−85.1±0.9	459±57	−38.7±2.1
cAMP+Pax.	WT	−83.2±1.2	565±52	−41.5±0.1
	β4 KO	−85.1±0.9	376±30	−35.2±3.2

Intrinsic membrane properties. Mean ± SE.